THE JOURNAL OF BIOLOGICAL CHEMISTRY
Vol. 274, No. 6, Issue of February 5, pp. 3407–3413, 1999

Printed in U.S.A.

The Family of Cold Shock Proteins of *Bacillus subtilis*

STABILITY AND DYNAMICS *IN VITRO* AND *IN VIVO**

(Received for publication, July 28, 1998, and in revised form, November 24, 1998)

Thomas Schindler‡§¶, Peter L. Graumann§‖, Dieter Perl‡, Saufung Ma‖‡‡, Franz X. Schmid‡, and Mohamed A. Marahiel‖**

From the ‡Laboratorium für Biochemie, Universität Bayreuth, 95440 Bayreuth and the ‖Biochemie, Fachbereich Chemie, Hans-Meerwein-Strasse, Philipps-Universität Marburg, 35032 Marburg, Germany

Bacillus subtilis **possesses three homologous small cold shock proteins (CSPs; CspB, CspC, CspD, sequence identity >72%). They share a similar β-sheet structure, as shown by circular dichroism, and have a very low conformational stability, with CspC being the least stable. Similar to CspB, CspC and CspD unfold and refold extremely fast in a N ⇌ U two-state reaction with average lifetimes of only 100–150 ms for the native state and 1–6 ms for the unfolded states at 25 °C. As a consequence of their low stability and low kinetic protection against unfolding, all three cold shock proteins are rapidly degraded by proteases *in vitro*. Analysis of the CSP stabilities *in vivo* by pulse-chase experiments revealed that CspB and CspD are stable during logarithmic growth at 37 °C as well as after cold shock. The cellular half-life of CspC is shortened at 37 °C, but under cold shock conditions CspC becomes stable. The proteolytic susceptibility of the CSPs *in vitro* was strongly reduced in the presence of a nucleic acid ligand, suggesting that the observed stabilization of CSPs *in vivo* is mediated by binding to their substrate mRNA at 37 °C and, in particular, under cold shock conditions.**

Cold shock proteins (CSPs)[1] are found in a wide range of Gram-positive and Gram-negative bacteria, often in families of three (as in *Bacillus subtilis*) to nine (as in *Escherichia coli*) highly homologous members (identity >70%) (for review see Ref. 1). Recently, CSPs were also found in *Aquifex aeolicus* (2) and *Thermotoga maritima* (3), indicating that CSPs were present at the origin of bacterial divergence and therefore are presumably an evolutionarily old class of proteins. A CSP-homologous domain (cold shock domain) is found in many eukaryotic nucleic acid-binding proteins (for review see Ref. 4), where it confers specific RNA binding (5, 6). CSPs bind to single-stranded DNA and RNA in a cooperative manner and with low sequence specificity (7–9). As a model for the cold shock domain, the structures of CspB (*B. subtilis*) and CspA (*E. coli*) were solved, revealing similar, compact five-stranded β-barrel folds (10–13). CSPs possess binding sites for single-stranded nucleic acids on their antiparallel three-stranded β-sheets, which involve basic and aromatic residues. These are the so-called RNA-binding ribonucleoprotein motifs (13, 14).

CSPs were discovered originally because they are strongly induced in response to cold shock (15), and thus they were assumed to be important for adaptation to low temperatures. The major cold shock protein, CspA from *E. coli*, was in fact shown to increase the synthesis of several cold stress-inducible proteins after a decrease in temperature (16). However, different members of the *E. coli* CSP family are regulated differently and appear to perform functions also during cell division or during the stationary phase (17). Recent work shows that in *B. subtilis,* CSPs are essential for protein synthesis at low as well as at optimal temperature and also during the stationary phase (8). Moreover, CspA from *E. coli* destabilizes secondary and tertiary structures in RNA *in vitro* (7), which led to the assumption that CSPs facilitate initiation of translation as "RNA chaperones" by preventing the formation of stable, nonproductive secondary structures in mRNA under various conditions.

Induction of CSPs after cold shock originates from an increase in transcription of their genes (18) and, to a greater extent, from the stabilization of their mRNAs (19, 20). In addition, the *cspA*-mRNA seems to be translated more efficiently than the mRNAs coding for proteins that are not induced by cold stress (21). Whether the concentration of CSPs is also regulated on the level of protein stability is not yet known. CspB from *B. subtilis* exhibits a very low conformational stability, and its native form exists in an extremely dynamic equilibrium with the unfolded form. The average lifetime of the folded conformation is only about 100 ms under physiological conditions. Therefore, we proposed that CspB might be subject to rapid degradation *in vivo* (22).

The three members of the CSP family from *B. subtilis* show sequence identities of 72–80% (Table I) and can complement each other *in vivo* (8). CspB is important both at low and at optimal temperatures. CspC functions mainly at low temperature and CspD mainly at optimal temperature.

Here we investigated the stability and the folding kinetics of CspC and CspD of *B. subtilis*. These two cold shock proteins resemble CspB in their rapid unfolding and refolding and in their low thermodynamic stability. Marginal stability linked with high conformational dynamics might be an effective means for regulating the cellular concentration of CSPs. To explore this possibility, we investigated the proteolytic stabilities of CspB, CspC, and CspD *in vitro*. The proteolytic susceptibility of all three proteins is in fact high but decreases strongly in the presence of substoichiometric amounts of single-stranded nucleic acids. *In vivo*, CspB and CspD, but not CspC,

* This work was supported by the Deutsche Forschungsgemeinschaft (SFB 395 and Schm 444/12-1), the Human Frontier Science Program, and the Fonds der Chemischen Industrie. The costs of publication of this article were defrayed in part by the payment of page charges. This article must therefore be hereby marked "*advertisement*" in accordance with 18 U.S.C. Section 1734 solely to indicate this fact.

§ These authors contributed equally to this work.
¶ Present address: The Rockefeller University, P. O. Box 3, Laboratories of Molecular Biophysics, 1230 York Ave., New York, NY 10021.
** To whom correspondence should be addressed: Biological Laboratories, Harvard University, Cambridge, MA 02138. Tel.: 617-495-0532; Fax: 617-495-9300; E-mail: graumann@fas.harvard.edu.
‡‡ Present address: Imperial College, Wolfson Laboratories, Dept. of Biochemistry, London SW7 2AZ, Great Britain.

[1] The abbreviations used are: CSP, cold shock protein; PAGE, polyacrylamide gel electrophoresis; CD, circular dichroism; CHAPS, 3-[(3-cholamidopropyl)dimethylammonio]-1-propanesulfonic acid.

were stable at 37 and at 15 °C. CspC was significantly stabilized after a cold shock. These findings suggest that CSPs are complexed with a nucleic acid ligand in the cell, under cold shock conditions as well as at 37 °C, and are thereby protected against proteolytic attack.

EXPERIMENTAL PROCEDURES

Cloning and Heterologous Expression of cspC and cspD—The *cspC* and *cspD* structural genes were amplified using polymerase chain reaction (95 °C for 30 s; 47 °C for 1 min during the first 5 cycles and 55 °C for 1 min during the following 30 cycles; and 72 °C for 1 min) employing primers 5′-GGGGTACCCCAAGATAGTATATACTGTGTGG-3′ and 5′-CCATCGATGGTTAAGCTTTTTGAACGTTAGCAGC-3′ for *cspC* and 5′-GGGGTACCCCAGTACTAGGAGGAATTAAGC-3′ and 5′-GCTCTAGAGCATCTCATCATCATGTATTGAG-3′ for *cspD*, respectively. The *cspC* fragment was cloned into pBluescript SK(−)II vector (Stratagene) using *Kpn*I and *Cla*I restriction endonucleases; *cspD* was blunt-ended using Klenow polymerase and cloned into *Eco*RV-digested pBluescript SK(−)II vector. Correct orientation of the *cspC* and *cspD* genes, respectively, was verified by sequencing. The resulting plasmids pcspC and pcspD, respectively, were transformed into *E. coli* K38 pGP1-2 (23). Cells were grown in rich medium with 50 μg/ml ampicillin and 40 μg/ml kanamycin at 30 °C until reaching an optical density of 0.7, shifted to 42 °C, and further incubated for 2 h. Cells were centrifuged, resuspended in ice-cold buffer G50 (20 mM Tris-HCl, pH 7.5, 2 mM EDTA, 2 mM dithioerythritol), and subjected to sonication.

Purification of CspB, CspC, and CspD—Cold shock proteins were purified according to a general method described by Schindelin *et al.* (24); however, the method was modified and extended. Cellular extracts were applied to anion exchange chromatography (Superperformance150–10 Fraktogel EMD TMAE-650 [S]) and separated by a 0–1 M NaCl gradient in Buffer A (6 mM Tris-HCl, pH 6.8, 2 mM dithioerythritol, 2 mM EDTA). CspB and CspC eluted at a concentration of 300 mM NaCl and CspD at 360 mM NaCl. Because at 400 mM NaCl several small proteins of *E. coli* eluted, only the first fractions containing CspD were taken for further purification. CSP-enriched fractions were pooled, freeze-dried, and dissolved in Buffer C (50 mM Tris-HCl, pH 7.8, 100 mM KCl). Size exclusion chromatography on HiLoad 16/60 Superdex^{TM} 75 prep grade using Buffer C and a flow rate of 1 ml/min resulted in peak elution of CspB after 86 ml, of CspC after 87 ml, and of CspD after 83 ml. Fractions that were >95% pure according to SDS-PAGE were pooled and subjected to hydrophobic interaction chromatography (butyl-Sepharose). After the addition of 0.67 volume of saturated ammonium sulfate, CSPs were loaded onto the matrix equilibrated in 40% ammonium sulfate, 50 mM potassium phosphate buffer, pH 7.0. The proteins were eluted with 50 mM potassium phosphate buffer, pH 7.0. The protein-containing fractions were pooled, dialyzed against decreasing concentrations of ammonium hydrogen carbonate, and lyophilized. Protein concentrations were assayed by the method of Bradford (25) and by absorption measurements. Molar absorption coefficients at 280 nm for CspB, CspC, and CspD were calculated from their corresponding amino acid composition to be 5690, 5690, and 6970 M^{-1} cm^{-1}, respectively.

Circular Dichroism Spectroscopy—Circular dichroism in the far- and near-UV range was measured at 25 °C in 20 mM potassium phosphate buffer, pH 7.0, for the native protein or in 7.2 M urea in 0.1 M sodium cacodylate HCl, pH 7.0, for the unfolded protein. Data were collected with an 0.2-mm step resolution, a time constant of 1 s, and a scan speed of 20 nm/min, using a Jasco J600 spectropolarimeter and cuvettes of a path length of 0.05 cm for far-UV and 1 cm for near-UV range.

Urea-induced Unfolding Transitions—Samples of CspB, CspC, and CspD were incubated at a concentration of 1.5 μM for 1 h at 25 °C in the presence of 0.1 M sodium cacodylate HCl, pH 7.0, and varying concentrations of urea. Fluorescence of samples was measured at 343 nm with a 5 nm bandwidth. Excitation wavelength was 280 nm (3 nm bandwidth). Experimental data were analyzed by assuming that the transition between the folded and unfolded conformation is a U ⇌ N two-state reaction and that the fluorescence emissions of the native and the unfolded protein depend linearly on the urea concentrations (26). A nonlinear least squares fit of the experimental data was used to obtain the Gibbs free energy of stabilization, ΔG_{stab}, as a function of the urea concentration (27). CspC and, to a lesser extent, CspD showed a slight tendency to stick to the walls of quartz cuvettes at very low concentrations of urea, leading to a higher error in the measured fluorescence under those conditions. The first data point(s) were therefore not used for the nonlinear least squares fit.

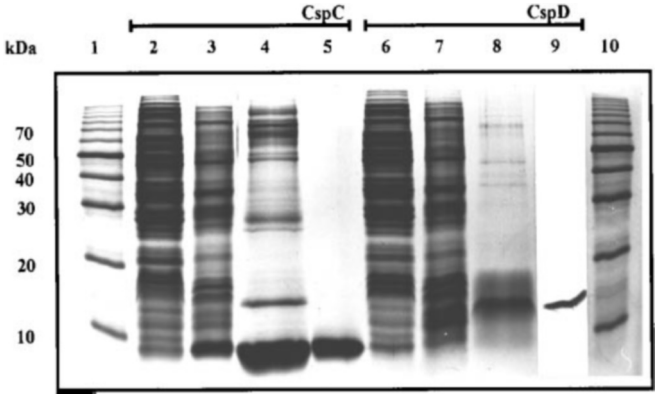

FIG. 1. **A Coomassie-stained 10% SDS-PAGE.** *Lanes 1* and *10,* 10-kDa protein ladder (Bio-Rad); *lanes 2* and *6,* whole cell extracts from K38 (pGP1–2 pcspC (*lane 2*) or pcspD (*lane 6*)) grown at 30 °C; *lanes 3* and *7*, whole cell extract from K38 (pGP1–2 pcspC (*lane 3*) or pcspD (*lane 7*)) shifted to 42 °C for 2 h; *lanes 4* and *8*, fractions containing peak elution of CspC and CspD, respectively, after anion exchange chromatography; *lanes 5* and *9*, fractions of CspC and CspD, respectively, after size exclusion chromatography.

Stopped-flow Kinetic Experiments—A DX17MV sequential mixing stopped-flow spectrometer (Applied Photophysics, Leatherhead, U.K.) was used for all kinetic measurements. The folding kinetics were followed by the change in fluorescence above 300 nm after excitation at 280 nm (10 nm bandwidth). The zero time point and the dead time of mixing were determined using the procedure suggested by Tonomura *et al.* (28). All unfolding and refolding experiments were carried out in 0.1 M sodium cacodylate HCl, pH 7.0. To initiate unfolding, typically 16 μM native protein was diluted 11-fold with buffers of varying urea concentrations to give final urea concentrations between 2.5 and 8.0 M. To initiate refolding, 16 μM unfolded protein in 5.9 M (CspC) or 7.6 M (CspB, CspD) urea was diluted 11-fold with aqueous buffer or with urea solutions of varying concentrations to give the desired final urea concentration. Kinetics were measured eight times under identical conditions, averaged, and analyzed as monoexponential functions using software provided by Applied Photophysics. Folding kinetics were analyzed on the basis of a U ⇌ N two-state folding reaction, where the measured rate constant λ is equal to the sum of the microscopic rate constants for refolding (k_{UN}) and unfolding (k_{NU}). Log k_{UN} and log k_{NU} are assumed to vary linearly with the concentration of urea. Values for the equilibrium constant K_{Stab} = [N]/[U] as a function of urea concentration were calculated from k_{UN}/k_{NU}.

Protease Digestion Assay—40 μM purified CspB, CspC, CspD, or hen egg white lysozyme were incubated in buffer (20 mM Tris-HCl, 5 mM $MgCl_2$, 50 mM NaCl, pH 8.6) containing 67 μg/ml trypsin at 25 °C in the presence or absence of 20 μM 54YB$^+$ single-stranded DNA (5′-GAATTCGCAGACGTGGGAATCCTACTGATTGGCCAAGGTGCTGGTGGTGTGTGG-3′). At various times (2, 4, 6, 10, 15, 30, 60, and 120 min), aliquots were withdrawn and subjected to SDS-PAGE. The Coomassie-stained gels were analyzed using a digital video camera (Gelprint 2000i from MWG-Biotech, Ebersberg, Germany), and the remaining amounts of full-length CSPs were quantified by using ONE-Dscan, version 1.0 (Scanalytics, Billerica, MA).

Pulse-Chase Labeling of Cellular Proteins and Two-dimensional Gel Electrophoresis—B. subtilis JH642 was grown in M9 minimal medium complemented with 0.01% yeast extract at 37 °C (29) to an optical density (600 nm) of 0.45 and labeled with 20 μCi of [^{35}S]methionine for 10 min or shifted to 15 °C for 5 min and then labeled for 30 min. A fraction was mixed with 0.1 volume of stop solution (10 mM Tris-HCl, pH 7.5, 1 mg/ml chloramphenicol) and incubated on ice before centrifugation. After washing with wash solution (10 mM Tris-HCl, pH 7.5, 0.1 mg/ml chloramphenicol), cells were frozen. The remaining culture was chased with a 50,000-fold excess of cold methionine. Samples were withdrawn after 10, 30, 60, 90, 120, and 180 min (37 °C) and after 1, 4, 8, 12, 24, and 36 h (15 °C). Cells were resuspended in Buffer B (10 mM Tris-HCl, pH 7.4, 1 mg/ml $MgCl_2 \times 6H_2O$; 50 μg/ml RNase A, 50 μg/ml DNase I, 100 μg/ml lysozyme; 243 μg/ml phenylmethylsulfonyl fluoride) and disrupted by sonication. After centrifugation, the supernatants were assayed for protein concentration according to Bradford (25), lyophilized, and resuspended in Buffer E (0.5 g of dithiothreitol, 2 g of CHAPS, 12.7 mg of phenylmethylsulfonyl fluoride, 27 g of urea, 2.5 ml of ampholytes, pH 3–10, and 30 ml of distilled H_2O (52 ml, final

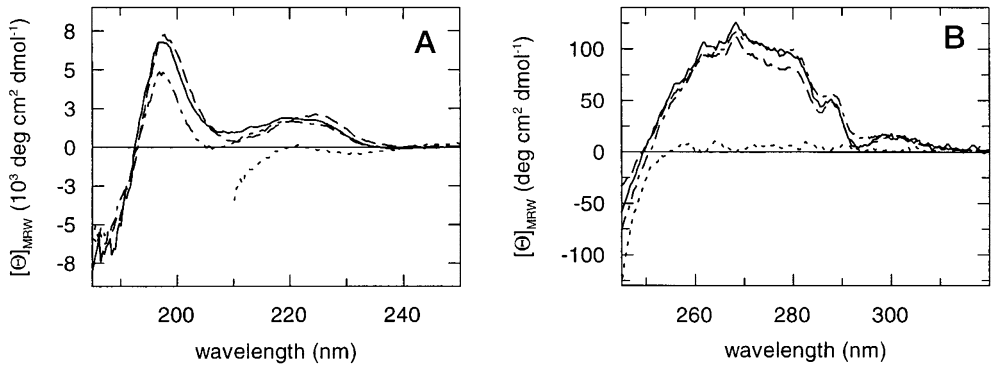

FIG. 2. **Circular dichroism spectra in far-UV (*A*) and near-UV (*B*) range of CspB (——), CspC (– - –), and CspD from *B. subtilis* (– –) recorded at 25 °C in 20 mM potassium phosphate buffer.** *Dotted line* shows control spectrum of CspB denatured in 7.2 M urea. The protein concentration was typically 40 μM.

TABLE I

Sequence alignment of the CSP protein family in B. subtilis

CspB is the reference molecule for this sequence alignment. Colons mark identical positions and points mark conservative exchanges. Ribonucleoprotein (RNP) motifs are in bold.

Protein	Sequence	%
	RNP1 RNP2	
CspD	MQNGKVKWFNNE**KGFGFIEV**EGGDD**VFVH**FTAIEGDGYKSLEEGQEVSFEIVEGNRGPQASNVVK-L	78[a]/85[b]
CspB	MLEGKVKWFNSE**KGFGFIEV**EGQDD**VFVH**FSAIQGEGFKTLEEGQAVSFEIVEGNRGPQAANVTKEA	
CspC	MEQGTVKWFNAE**KGFGFIER**ENGDD**VFVH**FSAIQSDGFKSLDEGQKVSFDVEQGARGAQAANVQK-A	71/79

[a] Identity with CspB.
[b] Similarity to CspB.

volume)) to yield equal concentrations of total proteins. Two-dimensional gel electrophoresis was performed as described by Graumann *et al.* (29).

RESULTS

Overproduction and Purification of CspC and CspD—CspC and CspD were overproduced employing the method of Tabor and Richardson (23) and purified by a method based on the procedure of Schindelin *et al.* (24) (see "Experimental Procedures"). It is apparent that CspC (7.2 kDa) migrates at a molecular mass of 8 kDa (Fig. 1, *lane 5*) and CspB migrates at 9 kDa (not shown), whereas CspD (7.2 kDa) migrates at 13 kDa (Fig. 1, *lane 9*). This discrepancy is caused by the effects of SDS, because in native PAGE, CspD (pI 4.32) and CspB (pI 4.31) comigrate, whereas CspC migrates more slowly because of the reduced negative charge (pI 4.53) (data not shown). UV spectra of purified protein fractions revealed absorbance maxima at 260 rather than 280 nm, which indicates that nucleic acids were still present. These residual, bound nucleic acids could be removed by hydrophobic interaction chromatography, resulting in UV spectra with shapes as expected from the chromophore composition of the CSPs and maxima at 280 nm (data not shown).

Structure and in Vitro Stability of CspC and CspD—The circular dichroism (CD) spectra of CspB, CspC, and CspD in the far- and near-UV region (Fig. 2) are very similar, indicating that the purified CSPs were properly folded and that, as expected from the high sequence homology (Table I), CspC and CspD resemble CspB in their three-dimensional structure. The ellipticity in the far-UV range is low because the CSPs lack α-helices. The CD maximum at 197 nm (Fig. 2*A*) originates from the antiparallel β-sheet structure of the CSPs. This maximum is slightly reduced in the CD spectrum of CspC because CspC is the least stable protein and is not completely folded under the conditions of Fig. 2 (see below). The CD in this region is extremely sensitive to non-native molecules because these molecules possess a pronounced minimum at 200 nm. CspD has a Phe residue at position 38 instead of a Tyr (as in CspB; see Table I). The minor differences in the near-UV CD may originate from this difference in sequence. Nevertheless, the close similarity among the CD spectra in Fig. 2 indicates that the differences in sequence between CspB, CspC, and CspD do not change the overall folded conformation.

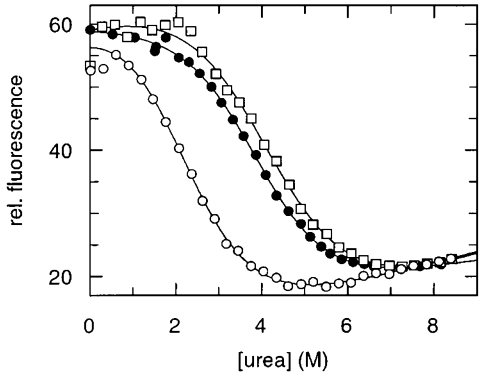

FIG. 3. **Urea-induced unfolding transitions of CspB (●), CspC (○), and CspD (□) in 0.1 M sodium cacodylate, pH 7.0, at 25 °C followed by change in fluorescence emission at 343 nm after excitation at 280 nm (CspC, CspD) or 295 nm (CspB).** The protein concentrations were 1.5 μM for CspC and CspD and 13.5 μM for CspB. The *continuous lines* represent least squares fit analyses of the experimental data based on a two-state U $\rightleftharpoons$ N unfolding mechanism. For resulting values for cooperativity (m) and Gibbs free energy (ΔG_{Stab}), see Table II. The data points of measured fluorescence of CspC and CspD at 0 M urea concentrations were not included in the fit (see "Experimental Procedures"). *rel.*, relative.

The urea-induced equilibrium unfolding transitions of the three CSPs, as monitored by the decrease in fluorescence emission of the single Trp residue at position 8, are shown in Fig. 3. With increasing concentrations of urea, the fluorescence intensities of all three CSPs decrease in single cooperative transitions. CspB and CspD show very similar stabilities. The midpoints of their unfolding transitions are at 3.9 M urea (CspB) and 4.1 M urea (CspD) (Table II). The conformational stability

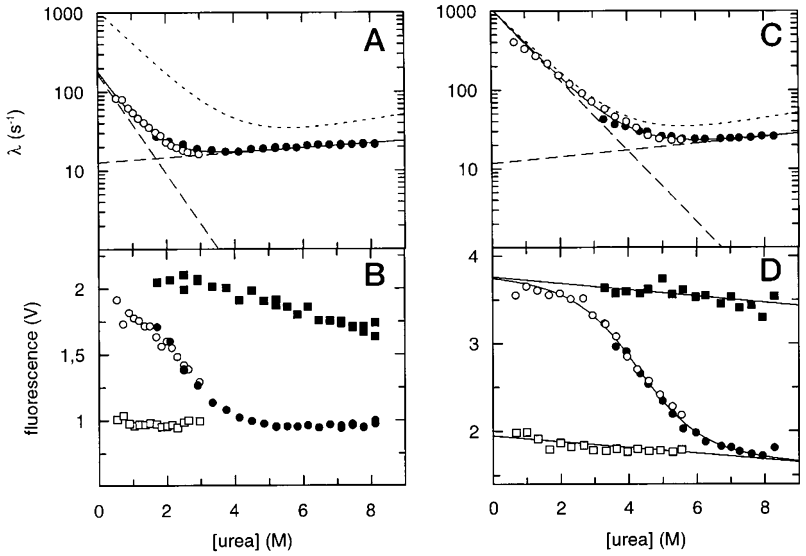

FIG. 4. **Dependence of unfolding (●, ■) and refolding (○, □) kinetics of CspC (*A, B*) and CspD (*C, D*) on concentration of urea in 0.1 M sodium cacodylate, pH 7.0, at 25 °C.** In *A* and *C*, the apparent rate constant is plotted as the function of urea concentration. *Continuous lines* in *A* and *C* represent the fit of the data according to a kinetic two-state mechanism, and *broken lines* give the calculated dependence of microscopic constants of velocity (*V*) of unfolding (k_{UN}) and refolding (k_{UN}) on concentration of urea (Table II). Kinetic analysis of CspB, taken from Ref. 27, is shown by *dotted lines*. *B* and *D* are plots of start (□, ■) and end points (○, ●) of kinetics. All points are averages of at least eight measurements. For CspD (*panel D*), the start and end points were also analyzed according to a two-state model, resulting in values for $\Delta G_{Stab}(H_2O)$ and *m* of −11.8 kJ/mol and 2.77 kJ/(mol·M), respectively. At 0 M urea, already 8% of the CspC molecules were unfolded, such that values for unfolding of CspC do not reflect the base line of the native protein.

TABLE II
Thermodynamic parameters for folding of CspB, CspC, and CspD

All data were determined at 25 °C in the presence of 0.1 M sodium cacodylate HCl, pH 7.0.

	Equilibrium unfolding[a]			Folding kinetics[b]					
	ΔG_{Stab} (H_2O)[c]	m[d]	$[urea]_{1/2}$[e]	k_{UN} (H_2O)[f]	k_{NU} (H_2O)[f]	ΔG_{Stab} (H_2O)[g]	m[h]	m_{UN} rel[i]	$[urea]_{1/2}$[e]
	kJ/mol	*kJ/(mol·M)*	*M*	S^{-1}	S^{-1}	*kJ/mol*	*kJ/(mol·M)*		
CspB	−11.4 ± 0.9	2.9 ± 0.2	3.9	1070 ± 20	12 ± 7	−11 ± 1.4	2.8 ± 0.3	0.86	3.9
CspC	−6.0 ± 0.9	3.0 ± 0.3	2.0	166 ± 11	11.7 ± 0.7	−6.6 ± 0.3	3.7 ± 0.2	0.94	1.8
CspD	−10.2 ± 1.0	2.5 ± 0.2	4.1	1083 ± 124	11.8 ± 2.8	−11.2 ± 0.9	2.8 ± 0.3	0.91	4.0

[a] The equilibrium data are from the analyses of the transitions shown in Fig. 3.
[b] The kinetic parameters are from the analyses of data in Fig. 4, *A* and *C*.
[c] ΔG_{Stab} (H_2O), Gibbs free energy in the absence of urea.
[d] *m*, dependence of ΔG_{Stab} on urea ($\partial \Delta G_{Stab}/\partial$[urea]).
[e] $[urea]_{1/2}$, midpoint of the urea-induced transition.
[f] $k(H_2O)$, microscopic rate constant of unfolding ($k_{UN}(H_2O)$) and folding ($k_{UN}(H_2O)$) in the absence of urea.
[g] ΔG_{Stab} (H_2O) as derived from the ratio of the microscopic rate constants of refolding and unfolding ($-RT\ln (k_{UN}(H_2O)/k_{UN}(H_2O))$.
[h] *m* as derived from the urea dependence of k_{UN} and k_{NU} ($-RT[(\partial \ln k_{UN}/\partial[urea]) - (\partial \ln k_{NU}/\partial[urea])]$).
[i] m_{UN} rel, fractional change of the *m* value during refolding ($m_{UN}/(m_{UN} - m_{NU})$).

of CspC is considerably lower. The midpoint of its transition is at 2 M urea (Fig. 3; Table II). For CspB, we have previously shown that the change in fluorescence reflects global unfolding of the β-barrel (22). The transitions in Fig. 3 were analyzed according to the linear two-state model (26). The resulting values for the Gibbs free energy of stabilization in the absence of a denaturing agent ($\Delta G_{Stab}(H_2O)$) are −11.4 kJ/mol for CspB and −10.2 kJ/mol for CspD (Table II), although the midpoint of the unfolding transition is slightly higher for CspD. This is a consequence of the small difference in cooperativity ($m = \partial \Delta G_{Stab}/\partial$[urea]) between the transition of CspD (m = 2.5 kJ/mol) and CspB (m = 2.9 kJ/mol). CspC is significantly less stable than CspB and CspD ($\Delta G_{Stab}(H_2O)$ = 6.0 kJ/mol; Table II). Thus, under native conditions, 8% of all CspC molecules are expected to be in an unfolded state, compared with 1% for CspB. The high percentage of unfolded CspC molecules was also apparent in its far-UV CD spectrum (see above).

Conserved Two-state Folding Mechanism for CSPs—The unfolding and refolding kinetics of CspC and CspD were measured after rapid 11-fold dilutions of the native and unfolded proteins, respectively, to various final concentrations of urea in a stopped-flow apparatus. As in the equilibrium unfolding experiments (Fig. 3), the folding kinetics were monitored by fluorescence. All kinetic curves could be well described by monoexponential functions. As observed previously for CspB, the unfolding of CspC and the unfolding of CspD are reversible two-state processes under all conditions, and identical values were obtained for the measured rate constants λ in unfolding and refolding experiments performed at the same concentration of denaturant in the transition regions (Fig. 4, *A* and *C*). Moreover, identical final fluorescence values were reached, irrespective of whether the kinetics started from the totally unfolded or the native protein, and these final values followed the equilibrium unfolding transitions (*cf.* Figs. 3 and 4, *B* and *D*). The initial fluorescence values of unfolding trace the base line for the native protein, and the initial values of refolding trace the base line of the unfolded protein (Fig. 4, *B* and *D*). There is no indication for rapid changes in fluorescence during the experimental dead time, and therefore partly folded intermediates seem not to accumulate before the rate-limiting event of folding. As found previously for CspB (22), the urea dependence of the apparent rate constants of folding (λ) of both CspC

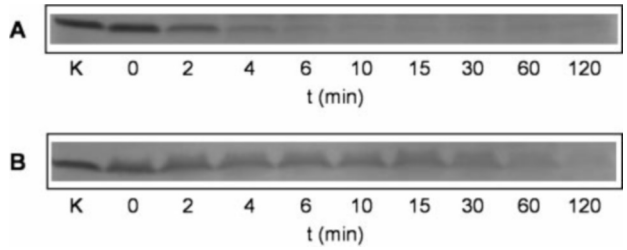

FIG. 5. **Tryptic digest of CspB (25 °C in 20 mM Tris-HCl, 5 mM $MgCl_2$, 6% glycerol, pH 8.6, 40 μM CspB, 67 μg/ml trypsin) in the absence (*A*) or the presence (*B*) of the single-stranded DNA 54YB$^+$ ligand (half the amount of CspB) followed by Coomassie-stained SDS-PAGE.** Aliquots were withdrawn at indicated times. The reaction was stopped by the addition of SDS sample buffer and immediate transfer to 95 °C. *K*, control (40 μM CspB, no trypsin).

and CspD, shown in Fig. 4, *A* and *C,* are very well described by the two-state model (U ⇌ N), where λ equals the sum of the microscopic rate constant of unfolding (k_{NU}) and refolding (k_{UN}) (λ = k_{UN} + k_{NU}). The refolding kinetics of CspD almost coincide with those of CspB (the *dotted line* in Fig. 4*C*), and the extrapolated rate constant of folding in the absence of urea (1080 s^{-1}) is virtually identical for the two proteins (Table II). CspC refolds more slowly than CspB and CspD (Fig. 4*C*). The rate constant of its refolding at 0 M urea is 6.5-fold decreased to 170 s^{-1}.

For all three proteins, the microscopic rate constants of unfolding are only marginally dependent on urea concentration, and they all extrapolate to a common value of 12 s^{-1} under native conditions in the absence of urea (Table II). This shows that the remarkably high frequency of unfolding under physiological conditions that was first noted for CspB is a conserved property of all three cold shock proteins.

The kinetic and equilibrium data (compared in Table II) are mutually consistent. This consistency indicates that the linear two-state model is an excellent representation for the folding transitions of all three cold shock proteins and that the fluorescence change in the equilibrium unfolding (Fig. 3) indeed reflects global unfolding.

Proteolytic Susceptibility of CSPs in Vitro—The low thermodynamic stability combined with the high conformational dynamics of all three CSPs should render them very sensitive to proteolytic digestion. To examine this possibility, we exposed CspB, CspC, CspD, and hen egg white lysozyme in a control experiment to 67 μg/ml trypsin at 25 °C. After various time intervals, samples were assayed by SDS-PAGE. The decrease of the intensity of the band for the intact protein with time is shown in Fig. 5*A* for CspB. All three CSPs were rapidly cleaved by trypsin, with half-times shorter than 5 min (Fig. 6). The half-time of degradation of lysozyme exceeded 2 h under the same conditions (Fig. 6*A*, *inset*). The protein with the lowest thermodynamic stability, CspC, is degraded most rapidly (Fig. 6*C*), as expected.

The cold shock proteins bind with high affinity to single-stranded DNA molecules containing ATTGG sequences, such as the 54YB$^+$ oligonucleotide (30). This DNA ligand protected the CSPs strongly against cleavage by trypsin (Figs. 5*B* and 6) although it was present only in a substoichiometric amount (20 μM) relative to the CSPs (40 μM) during the proteolysis. The half-lives of CspB and CspD increased more than 10-fold (Fig. 6, *A* and *B*). The stabilization of CspC was less pronounced but still significant (Fig. 6*C*), which is in agreement with earlier findings that CspC has a markedly reduced affinity for single-stranded DNA and RNA *in vitro* (8). The half-life of lysozyme did not change in the presence of 54YB$^+$ (*inset* in Fig. 6*A*).

Stability of CSPs in Vivo—The stabilities of CspB, CspC, and CspD *in vivo* in *B. subtilis* were determined by pulse-chase

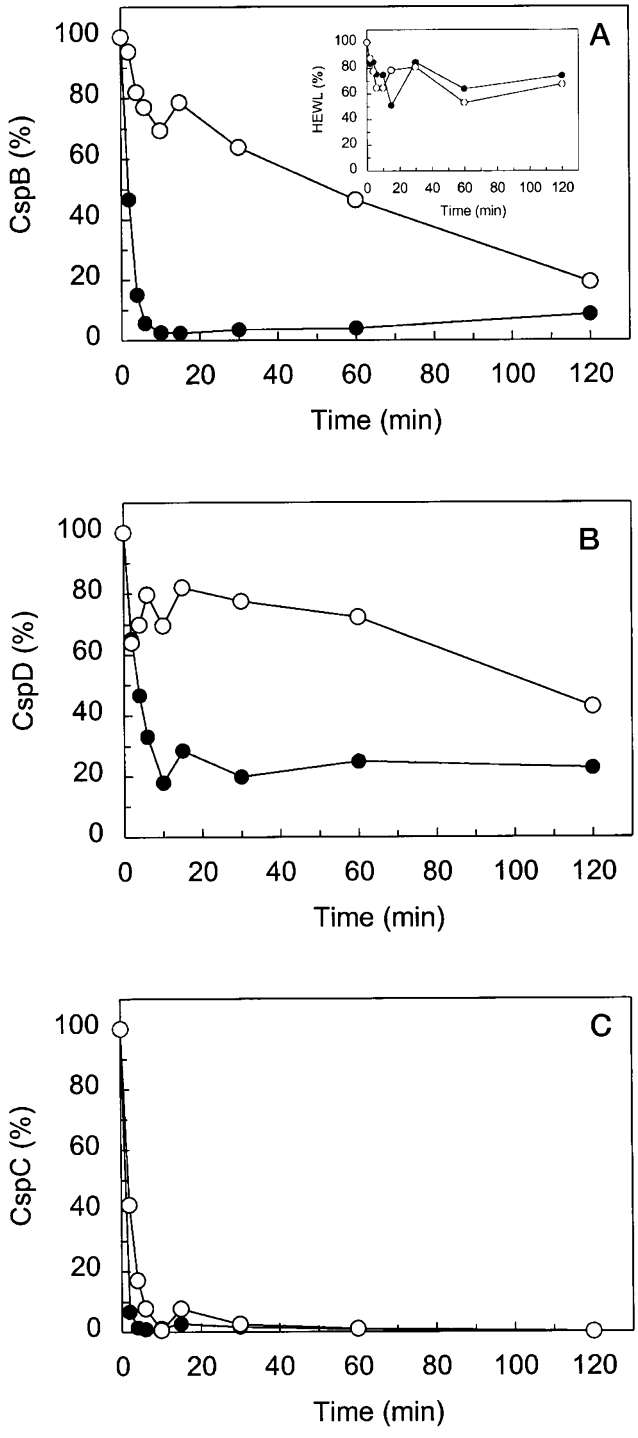

FIG. 6. **Time course of tryptic digest of CSPs (40 μM), CspB (*A*), CspD (*B*), and CspC (*C*) in the absence (●) or the presence (○) of 20 μM 54YB$^+$ single-stranded DNA.** Aliquots were withdrawn at the indicated time points and analyzed by SDS-PAGE (see Fig. 5). The kinetics of hen egg white lysozyme are shown as *inset* in *panel A*.

experiments. In minimal medium at 37 °C, the doubling time of JH642 was 108 min, which, after a cold shock to 15 °C, increased to 24 h (data not shown). From Fig. 7 it is apparent that at 37 °C, the amount of CspB and CspD was approximately 50% after 120 min compared with 0 min after pulse labeling (*panels A* and *B*). Thus, the half-lives of CspB and CspD correspond to the doubling time of logarithmically growing cells, similar to the majority of proteins synthesized during this period of growth (not shown). Representative for this group of proteins that are not subject to detectable degradation are

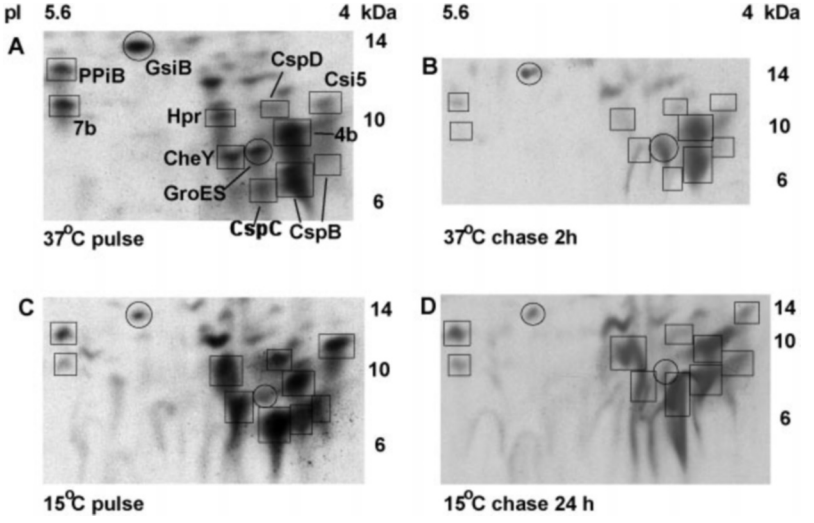

FIG. 7. **Lower acidic part of autoradiograms from 13.5% second dimension (SDS-PAGE) two-dimensional gels containing cellular extracts from [^{35}S]methionine-labeled *B. subtilis* JH642.** *A* and *B,* grown at 37 °C until midexponential phase (optical density at 600 nm (A_{600}) = 0.45). *A,* pulsed for 10 min; *B,* chased for 2 h. *C* and *D,* shifted at A_{600} = 0.45 from 37 to 15 °C. *C,* pulsed for 30 min; *D,* chased for 24 h. Equal amounts of proteins were subjected to two-dimensional gel electrophoresis. Identification of spots is taken from Refs. 29 and 34. CspB is present as formylated (more acidic spot) and deformylated protein under cold shock conditions (*C* and *D*).

GsiB, GroES, and spot 4b. Only a few proteins, such as PPiB, Hpr, and CheY, showed slight degradation with a half-life of approximately 90 min (Fig. 7, *A* and *B*). In contrast, CspC, Csi5, and spot 7b were no longer detectable after 120 min of chase (contrarily to 60 min after chase, not shown) and showed a half-life of approximately 75 min. Therefore, these proteins are detectably degraded during logarithmic growth.

After cold shock, synthesis of CspB, CspC, CspD, Csi5, CheY, and Hpr increased, whereas that of GsiB, GroES, and spot 7b decreased (Fig. 7, *A* and *C*) as reported previously (29). Twenty-four hours after the chase (corresponding to one doubling time), the levels of all cold stress-induced proteins (CIPs, including CSPs) and of most other proteins were about 50% of the levels after the pulse (Fig. 7, *C* and *D*). Degradation of CSPs was still not detectable 36 h after the pulse (not shown). These findings show that with the exception of a few proteins (such as CheY, Fig. 7, *C* and *D*), general protein degradation is low after cold shock to 15 °C.

The results show that in *B. subtilis,* CspB and CspD are stable at 37 °C as well as under cold shock conditions. CspC, however, is completely stable only after a drop in temperature to 15 °C. Thus, in contrast to their low barrier against unfolding and their pronounced protease sensitivity *in vitro*, CspB and CspD are stable molecules *in vivo*, even in the absence of a cold shock. This agrees with the finding that CSPs are essential at low temperatures as well as at 37 °C (8). We showed that CSPs are stabilized in the presence of a limiting amount of a nucleic acid ligand *in vitro,* and therefore, we propose that *in vivo* CSPs exist in a tight complex with their biological ligand (probably mRNA) and are thereby stabilized. This hypothesis is possible because mRNA is highly abundant in the bacterial cell and because CSPs bind cooperatively and rather nonspecifically to RNA *in vitro* (7, 8).

DISCUSSION

The CSPs of *B. subtilis* (CspB, CspC, CspD, sequence identity 71–78%) share a common three-dimensional structure (10–13). CspB folds extremely rapidly and reversibly without any intermediate steps and has a very low kinetic barrier to unfolding (22). Similarly rapid two-state unfolding and refolding kinetics were found also for CspC and CspD in this work. These properties are likely to be general features of CSPs, because recently they were also found for CSPs from other mesophilic, thermophilic, and hyperthermophilic bacteria (3, 31).

CspB and CspD of *B. subtilis* show virtually identical low thermodynamic stabilities of −10 to −11 kJ/mol, and the stability of CspC is further reduced to only −6 kJ/mol. As a result, 8% of CspC molecules are expected to be denatured even under native conditions, compared with 1% for CspB. Interestingly, in CspC, Pro-58 of CspB and CspD is replaced by alanine (Table I). This substitution probably contributes to the reduced conformational stability of CspC because Pro residues reduce the entropy of the unfolded protein. All three CSPs feature a highly dynamic native conformation. CspB and CspD show almost identical rates of unfolding (12 s^{-1}) and refolding (1000 s^{-1}). Refolding of CspC is decelerated 8-fold, which reflects its lowered stability, but it also unfolds at a rate of 12 s^{-1} under native conditions.

Consistent with their low thermodynamic stability and high frequency of unfolding, we found that all three CSPs of *B. subtilis* are excellent substrates for proteases *in vitro*. Their susceptibilities parallel the rank order of conformational stability; CspD is slightly more resistant to proteolytic degradation than CspB, whereas CspC with its particularly low thermodynamic stability is degraded most rapidly.

The pulse-chase experiments in Fig. 7 show that, despite this rapid proteolysis of the purified proteins *in vitro*, CspB and CspD are not detectably degraded during logarithmic growth of *B. subtilis* at 37 °C. This result is in agreement with the finding that the CSPs have an essential function at optimal temperature (8). CspC is degraded at 37 °C with a half-life of about 75 min. CspB and CspD are readily detectable in Coomassie stained SDS-PAGE from cells grown at 37 °C, whereas CspC is only faintly visible by Western blotting at this temperature (data not shown). After cold shock, all three CSPs were stable for at least 36 h (>1 doubling time). Thus, in the absence of a detectable turnover, enhanced synthesis following cold shock (29) leads to an increase in the intracellular concentrations of CSPs. The different *in vivo* CSP stabilities agree with earlier findings that the function of CspC is more important at low temperatures, whereas CspB performs its function, which is not transient, at optimal growth temperature as well as under cold shock conditions (8).

CspA of *E. coli* has also been reported to be stable after cold shock at 10 °C. For its stability at 37 °C, contradictory results have been obtained. Pulse labeling of cold-shocked cells followed by a chase at low temperature and subsequent shift to optimal growth temperature was reported to produce CspA that could still be detected after several hours at 37 °C (32). On the other hand, induction of *cspA* from a heterologous promoter and pulse-chase of CspA at 37 °C resulted in protein with a rather short half-life (7 min under the experimental conditions employed) (19).

Induction of CSPs by cold shock originates from increased transcription of *csp* genes and from stabilization of *csp* mRNAs (18–20). Our data show that the increase in the CspC concentration following a decrease in temperature is at least partly mediated by enhanced protein stability, revealing that CSP induction can also be achieved at the level of protein stability. The conformational stability of CspC is considerably lower than that of CspB and CspD and may account for efficient degradation of CspC at 37 °C. Following cold shock, the half-life of CspC may be prolonged by a reduction of the proteolytic activity in the cell and/or a higher conformational stability of CspC at low temperatures.

The CSPs are probably stabilized *in vivo* by the cooperative binding to their mRNA substrates (7, 8). Indeed, CspB and CspD were strongly stabilized against proteolysis *in vitro* by a single-stranded 54-mer DNA ligand. It is remarkable that the rates of proteolysis of CspB and CspD decreased more than 10-fold when the concentration of the DNA ligand was only half the CSP concentration. This finding suggests that several CSP molecules bind with strong positive cooperativity to a single-stranded DNA molecule and thus become protected against proteolytic cleavage. This binding by CSPs destabilizes double-stranded regions of RNA and thus increases their susceptibility to hydrolysis (7). Our results strongly suggest that even in the absence of a cold shock, CSPs are permanently complexed with nucleic acids, most likely with mRNA. On the other hand, the cellular concentration of CSPs can be efficiently controlled by the degradation of excess CSPs that are not bound to mRNA. A tight regulation of CSP levels appears to be important in bacteria, because heterologous induction of CspB in *E. coli* profoundly alters the pattern of protein synthesis and leads to a marked decrease in growth rate (33).

Acknowledgments—We thank Gabriele Schimpf-Weihland for continuous technical support and the members of the Schmid and Marahiel laboratories for many discussions. T. S. thanks the Jamaican national soccer team for determining the first authorship in the game against the Japanese national team.

REFERENCES

1. Graumann, P. L., and Marahiel, M. A. (1998) *Trends Biochem. Sci.* **23,** 286–290
2. Deckert, G., Warren, P. V., Gaasterland, T., Young, W. G., Lenox, A. L., Graham, D. E., Overbeek, R., Snead, M. A., Keller, M., Aujay, M., Huber, R., Feldman, R. A., Short, J. M., Olsen, G. J., and Swanson, R. V. (1998) *Nature* **392,** 353–358
3. Perl, D., Welker, C., Schindler, T., Schröder, K., Marahiel, M. A., Jaenicke, R., and Schmid, F. X. (1998) *Nat. Struct. Biol.* **5,** 229–235
4. Sommerville, J., and Ladomery, M. (1996) *FASEB J.* **10,** 435–443
5. Bouvet, P., Matsumoto, K., and Wolffe, A. P. (1995) *J. Biol. Chem.* **270,** 28297–28303
6. Matsumoto, K., Meric, F., and Wolffe, A. P. (1996) *J. Biol. Chem* **271,** 22706–22712
7. Jiang, W., Hou, Y., and Inouye, M. (1997) *J. Biol. Chem* **272,** 196–202
8. Graumann, P., Wendrich, T. M., Weber, M. H. W., Schröder, K., and Marahiel, M. A. (1997) *Mol. Microbiol.* **25,** 741–756
9. Mayr, B., Kaplan, T., Lechner, S., and Scherer, S. (1996) *J. Bacteriol.* **178,** 2916–2925
10. Schnuchel, A., Wiltscheck, R., Czisch, M., Herrler, M., Willimsky, G., Graumann, P., Marahiel, M. A., and Holak, T. A. (1993) *Nature* **364,** 169–171
11. Schindelin, H., Marahiel, M. A., and Heinemann, U. (1993) *Nature* **364,** 164–168
12. Schindelin, H., Jiang, W., Inouye, M., and Heinemann, U. (1994) *Proc. Natl. Acad. Sci. U. S. A.* **91,** 5119–5123
13. Newkirk, K., Feng, W., Jiang, W., Tejero, R., Emerson, S. D., Inouye, M., and Montelione, G. T. (1994) *Proc. Natl. Acad. Sci. U. S. A.* **91,** 5114–5118
14. Schröder, K., Graumann, P., Schnuchel, A., Holak, T. A., and Marahiel, M. A. (1995) *Mol. Microbiol.* **16,** 699–708
15. Jones, P. G., Van Bogelen, R. A., and Neidhardt, F. C. (1987) *J. Bacteriol.* **169,** 2092–2095
16. Jones, P. G., Krah, R., Tafuri, S., and Wolffe, A. P. (1992) *J. Bacteriol.* **174,** 5798–5802
17. Yamanaka, K., Fang, L., and Inouye, M. (1998) *Mol. Microbiol.* **27,** 247–256
18. Jiang, W., Jones, P., and Inouye, M. (1993) *J. Bacteriol.* **175,** 5824–5828
19. Brandi, A., Pietroni, P., Gualerzí, C. O., and Pon, C. L. (1996) *Mol. Microbiol.* **19,** 231–240
20. Goldenberg, D., Azar, I., and Oppenheim, A. B. (1996) *Mol. Microbiol.* **19,** 241–248
21. Jones, P. G., and Inouye, M. (1996) *Mol. Microbiol.* **21,** 1207–1218
22. Schindler, T., Herrler, M., Marahiel, M. A., and Schmid, F. X. (1995) *Nat. Struct. Biol.* **2,** 663–673
23. Tabor, S., and Richardson, C. C. (1985) *Proc. Natl. Acad. Sci. U. S. A.* **82,** 1074–1078
24. Schindelin, H., Herrler, M., Willimsky, G., Marahiel, M. A., and Heinemann, U. (1992) *Proteins Struct. Funct. Genet.* **14,** 120–124
25. Bradford, M. M. (1976) *Anal. Biochem.* **136,** 248–254
26. Santoro, M. M., and Bolen, D. W. (1988) *Biochemistry* **27,** 8063–8068
27. Schindler, T., and Schmid, F. X. (1996) *Biochemistry* **35,** 16833–16842
28. Tonomura, B., Nakatani, H., Ohnishi, M., Yamaguchi-Ito, J., and Hiromi, K. (1978) *Anal. Biochem.* **84,** 370–383
29. Graumann, P., Schröder, K., Schmid, R., and Marahiel, M. A. (1996) *J. Bacteriol* **178,** 4611–4619
30. Graumann, P., and Marahiel, M. A. (1994) *FEBS Lett.* **338,** 157–160
31. Reid, K. L., Rodriguez, H. M., Hillier, B. J., and Gregoret, L. M. (1998) *Protein Sci.* **7,** 470–479
32. Goldstein, J., Pollitt, S., and Inouye, M. (1990) *Proc. Natl. Acad. Sci. U. S. A.* **87,** 283–287
33. Graumann, P., and Marahiel, M. A. (1997) *Mol. Gen. Genet.* **253,** 745–752
34. Antelmann, H., Bernhardt, J., Schmid, R., Mach, H., Völker, U., and Hecker, M. (1997) *Electrophoresis* **18,** 1451–1463